

*Rapid communication***Few-cycle optical waveform synthesis**A. Poppe^{1,*}, R. Holzwarth², A. Apolonski^{1,3}, G. Tempea¹, Ch. Spielmann¹, T.W. Hänsch², F. Krausz¹¹Institut für Photonik, Technische Universität Wien, Gusshausstrasse 27, 1040 Wien, Austria²Max-Planck-Institut für Quantenoptik, Hans-Kopfermann-Strasse 1, 85748 Garching, Germany³Institute of Automation and Electrometry, SB RAS, Novosibirsk 630090, Russia

Received: 23 November 2000/Published online: 13 December 2000 – © Springer-Verlag 2000

Abstract. We demonstrate cycle-slip-free electronic control of the carrier-envelope phase evolution of few-femtosecond light pulses, optical access to its sub-cycle fluctuations and suppression of the amplitude noise of a mode-locked laser by phase control. As a result, few-cycle light waveforms can now be synthesized with electric and magnetic fields reproducible to within a known phase error (< 0.3 rad) and an unprecedentedly low amplitude error ($< 3\%$). The exploration of phase-sensitive light–matter interactions can be tackled.

PACS: 42.65.Re; 42.65.Ky; 42.25.Bs; 32.80.-t; 52.35.Mw

The synthesization of electromagnetic waveforms can be routinely accomplished by radio-frequency (rf) signal generators but has not been feasible in the optical region so far. Extending this capability to light frequencies by generating few-cycle light waves with a reproducible evolution of the electric and magnetic fields would, beyond its fundamental significance, open the door for unprecedented control of the evolution of ultrafast microscopic processes on a time scale of the light oscillation period [1].

Phase-coherent locking of beat notes of a mode-locked laser to radio-frequency (rf) local oscillators has recently allowed direct electronic control of both the repetition rate f_r and the carrier-envelope-offset frequency f_{ceo} , which not only resulted in a simple and powerful ‘frequency ruler’ with lines at $f_{ceo} + n f_r$ spanning a full octave [2–4] but also offered the potential for reproducible optical waveform synthesis in the time domain. In this work we exploit this potential for the first time.

Whereas laser mode locking is capable of generating a pulse train $E_n(t) = A_n(t) \exp(-i\omega_0 t + i\varphi_n) + \text{c.c.}$ with a nearly identical complex envelope $A_n(t)$ ¹ of the electric field $E_n(t)$, i.e. $A_{n+k}(t) \approx A_n(t)$, it is not able to stabilize the carrier-envelope phase φ_n [5]. This is because a pulse-to-pulse shift $\Delta\varphi_n$, arises from a difference between the

round-trip phase and group delay in the laser, which is subject to minor variations, $\Delta\varphi_n = \Delta\varphi_0 + \delta_n$, resulting in

$$\varphi_n = \varphi_0 + \sum_{k=1}^n \Delta\varphi_k = \varphi_0 + n\Delta\varphi_0 + \sum_{k=1}^n \delta_k. \quad (1)$$

The deviation of φ_n from the predictable value $\varphi_0 + n\Delta\varphi_0$ may accumulate to many times 2π over extended measurement times $T_m \gg f_r^{-1}$. Owing to the relationship $f_{ceo} = (\Delta\varphi/2\pi) f_r$ [6–8], phase locking of f_{ceo} can substantially reduce this random deviation. Whereas the avoidance of cycle slips of the stabilized beat notes with respect to rf clocks warrants stable optical frequency synthesis, the requirement for reproducible waveform synthesis is much more stringent: the carrier-envelope phase jitter

$$\sigma_\varphi(T_m) = \langle (\varphi_n - \varphi_0 - n\Delta\varphi_0)^2 \rangle_N^{1/2} \quad (2)$$

(where the angle brackets denote the average over $N = f_r T_m$) must not exceed a tiny fraction of π . *This requirement was not addressed before* and is the focus of this paper. The extent to which it can be fulfilled determines the feasibility of generating reproducible light waveforms at predictable instants.

In this paper, we report the emergence of this new experimental capability owing to: (i) full electronic control of the evolution of φ_n without cycle slips over extended periods of time in a few-femtosecond pulse train; (ii) measurement of σ_φ with a sub-cycle precision; and (iii) suppression of the amplitude noise of a mode-locked laser by means of phase control. This is achieved by exploiting optical nonlinearities for both closing the servo loop and as a diagnostic tool, for determining the sub-cycle jitter of φ_n , which is indispensable for a reproducible waveform generation. As a result, we demonstrate the generation of 5.8-fs light pulses (at $\lambda_0 \approx 0.8 \mu\text{m}$, where the field oscillation period is ≈ 2.7 fs) with their carrier-envelope phase locked to within 0.3 rad of an electronic oscillator and their field amplitude stabilized to within 3% for extended periods of time. Although φ_0 is still unknown, few-cycle light waveforms can be reproducibly synthesized for the first time, creating ideal conditions for measuring φ_0 by phase-sensitive nonlinear effects [1].

*Corresponding author.

¹ $A_n(t) = |A_n(t)|e^{-i\gamma(t)}$ accounts for amplitude and possibly frequency modulation with the chirp $\gamma(t)$ being a nonlinear function of t .

Figure 1 shows the schematic of our optical pulse generator. In contrast with previous work [2–4], the mode-locked spectrum emitted by a Ti:sapphire oscillator is broadened in a standard (rather than photonic-crystal) single-mode fiber to span more than an octave (500–1100 nm). Chirped mirrors compress the pulses exiting the fiber [9], hence the system delivers sub-6-fs pulses (see right inset in Fig. 4 and left inset in Fig. 6) with a peak power exceeding 1 MW at a repetition rate of 24 MHz. The wings of the spectrum (left inset in Fig. 4) extend from 500 to 1100 nm, spanning a full octave. A dichroic chirped mirror in the compressor (CM4 in Fig. 2) transmits the spectral components near 1080 nm and 540 nm towards a nonlinear interferometer generating the carrier-slip beat signal, which is schematically illustrated in Fig. 2. A dichroic mirror (DM) transmits the infrared components at 1080 nm, which are frequency-doubled in a 1-mm-thick BBO crystal and recombined with the 540-nm beam propagating through the other arm of the Mach–Zender interferometer at the beam splitter (BSP; SM represents the silver-coated steering mirrors). The spatial and temporal overlap of the two wave packets are ensured by the telescope formed by the lenses L1–2 and by the wedged glass plates W3–4, respectively. Interference between the orthogonally polarized 540-nm wave packets is enforced by a polarizer (P) aligned to yield a maximum beat signal at f_{ceo} . The optimized carrier-slip beat signal exhibits an improved signal-to-noise ratio (> 30 dB in a 100 kHz bandwidth), as compared to our previously used setup [9].

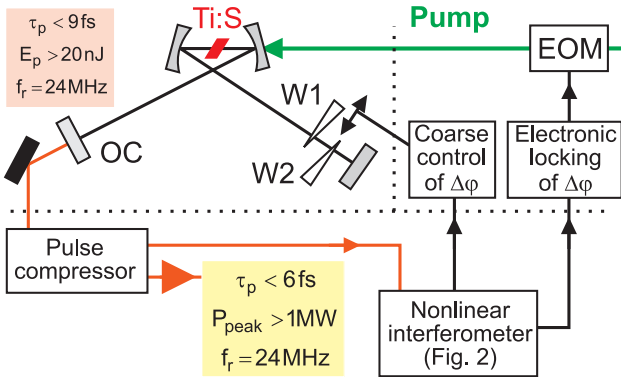


Fig. 1. Schematic of the few-cycle optical pulse generator and the servo loop used for carrier-envelope phase locking

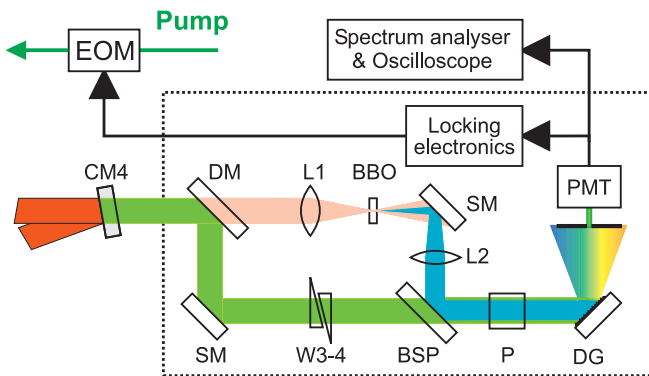


Fig. 2. Schematic of the optical setup used for generating the carrier-slip beat signal at ≈ 540 nm (for explanations see text)

We have phase locked the carrier-slip beat note to $f_{\text{local}} = 1$ MHz (synthesized by a stabilized local oscillator) by adjusting the pump power with an electro-optic modulator (EOM) [4]. This servo loop relies on nonlinearities (Kerr phase shift, Raman frequency shift [5]) translating a minor change of W into a significant change of $\Delta\varphi$ and hence that of f_{ceo} , as shown in Fig. 3. Once f_{ceo} is manually adjusted by translating a thin fused-silica wedge (W2 in Fig. 1) to be within $f_{\text{local}} \pm 100$ kHz, the servo loop pulls f_{ceo} to f_{local} and phase-locks the carrier-slip beat note to the signal of the local oscillator. The rf spectrum of the in-lock carrier-slip beat note is shown in Fig. 4, depicting the average of 20 scans. With the loop interrupted, f_{ceo} fluctuates over the full frequency range shown in Fig. 4 during the same measurement time (≈ 10 s).

Measurement of the ratio of the frequency of the in-lock carrier-slip beat signal to that of the local oscillator with a two-channel frequency counter yields no deviation of f_{ceo} from f_{local} to within the gate-time-limited resolution of 100 mHz up to the maximum gate time of $T_m = 10$ s allowed by our frequency counter. This implies that the servo loop suppresses the carrier-envelope phase jitter to $\sigma_\varphi < 2\pi$ for $T_m \geq 10$ s, i.e. φ_n is locked to the signal of the local oscillator firmly enough to prevent uncontrolled cycle slips from occur-

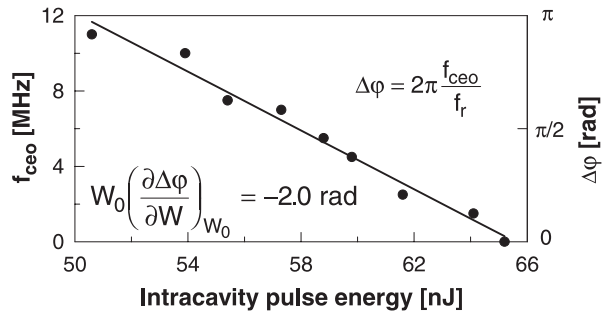


Fig. 3. Measured dependence of the carrier-envelope offset frequency f_{ceo} (and the pulse-to-pulse phase shift $\Delta\varphi$) on the intracavity pulse energy W (dots) and a linear regression to the depicted experimental data

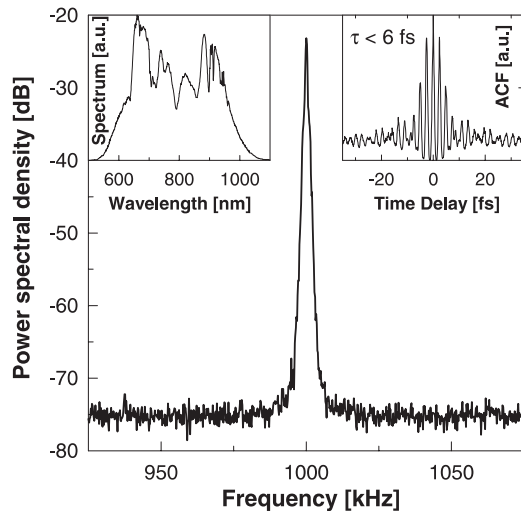


Fig. 4. Power spectral density of the in-lock carrier-slip beat signal at 540 nm recorded with a 1-kHz-resolution bandwidth. Spectrum (left inset) and interferometric autocorrelation (right inset) of the pulses exiting the pulse compressor consisting of the single-mode fiber SMF and chirped mirrors

ring. It is important to note that this degree of control can be achieved *without stabilizing f_r to an rf oscillator*. Minor variations in f_r merely shift the instants at which a pulse exits the laser without affecting phase locking, because the latter is performed at $f_{\text{local}} \ll f_r$ and is hence incapable of resolving this event. With f_r ‘freely floating’ merely the absence of synchronism of the pulse train with f_{local} has some negative implication. The selection of phase-stable pulses from the train by triggering the pulse picker using the local oscillator is tainted with a ‘sampling’ uncertainty of $\delta\varphi_{\text{error}} \leq 2\pi(f_{\text{ceo}}/f_r)$ due to desynchronism. This source of carrier-envelope phase uncertainty can be fully eliminated by simply deriving f_{local} from f_r via frequency division, *without the need for stabilizing f_{ceo} and f_r separately*.

As discussed above, cycle-slip-free operation is necessary but not sufficient for synthesizing reproducible waveforms in the time domain. To gain direct optical access to the sub-cycle jitter of φ_n , we utilize the fact that the parameter primarily controlled by the servo loop, namely the pulse energy W_n : (i) can be directly and permanently monitored; and (ii) is directly connected to $\Delta\varphi_n$ (see Fig. 3). As a consequence, the carrier-envelope phase jitter $\sigma_{\varphi(W)}$ that accumulates over T_m due to (controlled or random) variation of W_n can be determined from the power spectral density $S_W(f)$ of pulse energy variations [5] as

$$\sigma_{\varphi(W)}(T_m) = \frac{W_0}{\sqrt{2\pi}} \left| \frac{\partial \Delta\varphi}{\partial W} \right|_{W_0} \left(\int_{1/T_m}^{f_r/2} S_W(f) \frac{f_r^2}{f^2} df \right)^{1/2}, \quad (3)$$

where W_0 is the average intracavity pulse energy and we have made use of the approximately linear dependence of $\Delta\varphi$ on $\Delta W/W$ with a slope of $W_0 |\partial \Delta\varphi / \partial W|_{W_0} = 2 \text{ rad}$ at $W_0 = 60 \text{ nJ}^2$. The higher weight of low-frequency contributions to $\sigma_{\varphi(W)}$ is due to the increased time over which a deviation with frozen sign can accumulate.

Figure 5 depicts the measured $S_W(f)$ at low frequencies and the calculated $\sigma_{\varphi(W)}(T_m)$ for phase-locked as well as unlocked operation. The increase of $\sigma_{\varphi(W)}$ with T_m well beyond 2π for $T_m < 1 \text{ s}$ can be reconciled with the observation of cycle-slip-free operation (over periods of $T_m \geq 10 \text{ s}$) by assuming substantial carrier-envelope phase jitter originating from effects other than pulse energy fluctuations below frequencies of several tens of Hz. Hence, in this range a significant fraction of the pulse energy fluctuations have to be ‘rephased’ by the control loop to compensate a jitter from other sources and $\sigma_{\varphi(W)}$ mirrors this jitter.

Although the phase jitter originating from effects other than energy noise rapidly increases with T_m up to our longest measurement times (see upper thick grey line in Fig. 5), energy-noise-induced phase jitter becomes vastly dominant for $T_m > 1 \text{ s}$, as indicated by the dramatic noise reduction under locked conditions at frequencies below 1 Hz. This leads to a root mean square of the residual pulse energy fluctuations of $\sigma_W \approx 0.01\%$ over the spectral range 0.1 Hz – 0.1 MHz at the output of the carrier envelope-phase-locked oscillator,

² $\sigma_{\varphi(W)}$ here is defined in the same way as σ_φ in (2) except that perturbations to φ here results, by definition, from pulse energy fluctuations only. Expression (3) is obtained by replacing in (3) of [5] the lower boundary of integration with $1/T_m$, rather than the higher boundary, as mistakenly stated in the context of Fig. 3 in [5].

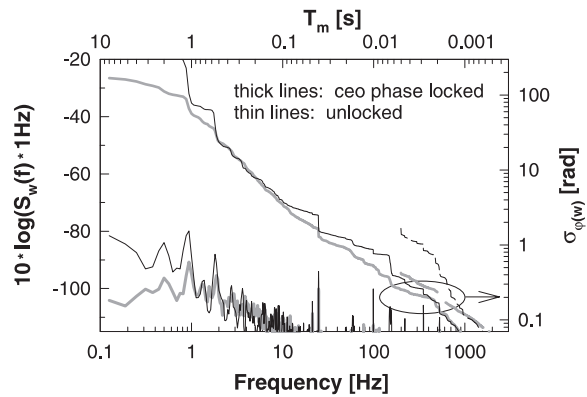


Fig. 5. Lower traces: Power spectral density $S_W(f)$ of the pulse energy fluctuations or its controlled variations at the output of the sub-10-fs Ti:sapphire laser with the servo loop interrupted (thin black line) and closed (thick grey line), shown for $f < 10 \text{ Hz}$, where the two spectra conspicuously deviate. Upper traces: Carrier-envelope phase jitter $\sigma_{\varphi(W)}$ as a function of T_m introduced by pulse energy variations, with the servo loop interrupted (thin black full and dashed lines) and closed (thick grey full and dashed lines), as calculated from (3) by using the respective $S_W(f)$. The dashed lines represent $\sigma_{\varphi(W)}(T_m)$ obtained from a different data set, recorded with a somewhat ‘noisier’ laser. Nevertheless, the servo loop suppresses the phase jitter (by dampening the energy fluctuations) to a comparable level as in the ‘quiet’ laser (full lines), providing evidence for the robustness of phase locking. The arrow indicates the phase jitter level ($\approx 0.2 \text{ rad}$) at which the servo loop starts responding

which is, to our knowledge, an unprecedented value. This is enhanced by somewhat less than a factor of 10 at the fiber output (due presumably to mechanically induced beam pointing instabilities at the fiber input), resulting in a reproducibility of the field amplitudes to within less than 3% in the sub-6-fs pulse train.

As compared to the sub-Hz regime, smaller but clearly notable and reproducible dampening of pulse energy fluctuations is caused by the servo loop in the sub-kHz range, as is evident from a corresponding suppression of $\sigma_{\varphi(W)}$, indicating the dominance of energy noise in this range. In repeated measurements (see also the dashed lines), $\sigma_{\varphi(W)}$ gets reproducibly suppressed at frequencies where it approaches $\approx 0.3 \text{ rad}$ for increasing T_m . The highest frequency at which the suppression of $\sigma_{\varphi(W)}$ sets in has ranged from 500 Hz to 1000 Hz in our experiments, depending on the relevant noise level (with the loop opened), which has varied somewhat in repeated measurements. Because energy-noise-induced jitter appears to dominate for $T_m < 10 \text{ ms}$, from these observations we may infer that the jitter of the carrier-envelope phase is kept safely below 0.3 rad by the servo loop. This value is comparable to $\delta\varphi_{\text{error}} \approx \pi/12$ and it will be interesting to see, whether the carrier-envelope phase jitter can be further lowered by deriving f_{local} from f_r in the future.

Using the SPIDER technique [10] for determining the amplitude envelope and frequency chirp, we can determine the range of waveforms our light generator can ‘synthesize’ reproducibly at regular times. The full line depicts such a waveform in Fig. 6, which is reproduced within the thickness of the line in each pulse following the trigger edge of a clock signal from the local oscillator. Shifting the phase of this trigger edge with respect to the signal controlling the servo loop results in a corresponding shift of the carrier with respect to the amplitude envelope.

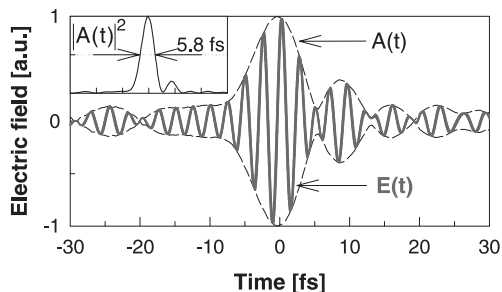


Fig. 6. Electric field $E(t) = A(t) \exp[-i\omega_0 t + i\varphi] + \text{c.c.}$ of a waveform (*full line*) emitted by our carrier-envelope-phase-locked few-cycle pulse generator at a particular setting of the trigger phase from the local oscillator yielding $\varphi = 1.25$ rad [$\gamma(0) = 0$], as obtained from a SPIDER measurement. The intensity envelope $I(t) \propto A(t)^2$ in the *inset* has a half-width of 5.8 fs. Contrasting this with the computed 3.5-fs duration of the pulse in the absence of phase errors indicates the presence of a significant chirp $\gamma(t)$ carried by the electric field oscillations. The waveform is reproduced with an accuracy represented by its thickness at a repetition rate of $f_{\text{focal}} = 1$ MHz.

lope (and chirp). Although the absolute phase is still unknown and hence no definite relation between the trigger phase and a particular waveform can be established, the presented optical waveform generation, due to its unique reproducibility, opens the door for exploring nonlinear optical effects sensitive to the absolute phase φ [1]. In spite of the similarities in the techniques applied *no previous experimental work warrants these claims*, indicating the need for a different approach to synthesizing frequencies and waveforms.

Upon their observation, phase-sensitive nonlinear optical effects can immediately be exploited for determining the absolute value of φ and assigning it to the corresponding

trigger phase in the demonstrated few-cycle waveform generator. This step will, in combination with shaping the amplitude envelope and tailoring the chirp using frequency-domain techniques [11], allow the synthesis of few-cycle light with arbitrary waveforms. Extending this capability from radio frequencies to the optical regime opens up new prospects in a number of fields where light is used for triggering, tracing and controlling microscopic processes.

Acknowledgements. The SPIDER measurements of M. Laubscher, A. Müller and B. Bacovic are gratefully acknowledged. This research has been sponsored by the Austrian Science Fund, Grants Y44-PHY and F016, as well as by INTAS, Grant 97-1058.

References

1. T. Brabec, F. Krausz: *Rev. Mod. Phys.* **72**, 545 (2000)
2. S.A. Diddams, D.J. Jones, J. Ye, S.T. Cundiff, J.L. Hall, J.K. Ranka, R.S. Windeler, R. Holzwarth, T. Udem, T.W. Hänsch: *Phys. Rev. Lett.* **84**, 5102 (2000)
3. D.J. Jones, S.A. Diddams, J.K. Ranka, A. Stentz, R.S. Windeler, J.L. Hall, S.T. Cundiff: *Science* **288**, 635 (2000)
4. R. Holzwarth, T. Udem, T.W. Hänsch, J.C. Knight, W.J. Wadsworth, P.S.J. Russell: *Phys. Rev. Lett.* **85**, 2264 (2000)
5. L. Xu, C. Spielmann, A. Poppe, T. Brabec, F. Krausz, T.W. Hänsch: *Opt. Lett.* **21**, 2008 (1996)
6. J.N. Eckstein: Ph.D. dissertation (Stanford University 1978)
7. H.R. Telle, G. Steinmeyer, A.E. Dunlop, J. Stenger, D.H. Sutter, U. Keller: *Appl. Phys. B* **69**, 327 (1999)
8. J. Reichert, R. Holzwarth, T. Udem, T.W. Hänsch: *Opt. Commun.* **172**, 59 (1999)
9. A. Apolonski, A. Poppe, G. Tempea, Ch. Spielmann, T. Udem, R. Holzwarth, T.W. Hänsch, F. Krausz: *Phys. Rev. Lett.* **85**, 740 (2000)
10. I. Walmsley, V. Wong: *J. Opt. Soc. Am. B* **13**, 2453 (1996)
11. A.M. Weiner: *Rev. Sci. Instrum.* **71**, 1929 (2000)